P-10

N94-23259

Improved Thermal Force Modeling for GPS Satellites

Y. Vigue
Tracking Systems and Applications Section

R. E. Schutz and P. A. M. Abusali
Center for Space Research, University of Texas, Austin, Texas

Geophysical applications of the Global Positioning System (GPS) require the capability to estimate and propagate satellite orbits with high precision. An accurate model of all the forces acting on a satellite is an essential part of achieving high orbit accuracy. Methods of analyzing the perturbation due to thermal radiation and determining its effects on the long-term orbital behavior of GPS satellites are presented. The thermal imbalance force, a nongravitational orbit perturbation previously considered negligible, is the focus of this article. The Earth's shadowing of a satellite in orbit causes periodic changes in the satellite's thermal environment. Simulations show that neglecting thermal imbalance in the satellite force model gives orbit errors larger than 10 m over several days for eclipsing satellites. This orbit mismodeling can limit accuracy in orbit determination and in estimation of baselines used for geophysical applications.

I. Introduction

Mismodeling of satellite force parameters can have a significant effect on satellite orbits, especially in orbit prediction [1]. Some applications require the capability to estimate and propagate satellite orbits with high precision. TOPEX/POSEIDON precision orbit determination, for example, requires precise modeling of nongravitational forces to fulfill mission requirements [2]. In addition, some of the observed drag and orbit decay on the Laser Geodynamics Satellite (LAGEOS) spacecraft have been attributed to unmodeled thermal forces [3,4]. To achieve a high level of orbit accuracy, an accurate model of all the forces acting on an Earth-orbiting satellite is necessary.

The focus of this analysis was to assess the effects on satellite orbits of neglecting thermal reradiation and of mismodeling nongravitational forces. Radiative heat transfer between a satellite and its environment is the basis for the thermal force model. A satellite in Earth orbit is continuously illuminated by radiation, most of which comes from the sun. The thermal imbalance force is directly related to the temperature distribution of the satellite in its changing environment. An uneven temperature distribution causes surfaces to reradiate energy at different rates. Some studies have shown that most of the thermal gradient forces on the TOPEX/POSEIDON satellite originate within the spacecraft body [2]. Other analyses have shown that the dominant source for thermal reradiation forces on a Global Positioning System (GPS)-like satellite is the solar panels, due to their large exposed area and low heat capacity [5]. The satellite's heated body reradiates energy at a rate proportional to its temperature, losing the energy in the form of photons. By conservation

of momentum, a net momentum flux out of the body creates a reaction force against the radiating surface, and the net thermal force can be observed as a small perturbation that affects long-term orbital behavior of the spacecraft [5]. The partial differential equations and boundary conditions describing the temperature distribution and the heat transfer between surfaces, along with the application of the finite element method, are presented in this article. A brief description of the statistical estimation technique used for studying the effect of the thermal imbalance force on satellite orbits is included.

II. Radiation and Heat Conduction Formulation

Two types of heat transfer that affect a spacecraft's orbit are radiation and heat conduction. The exchange of energy between the spacecraft and its surroundings is described by radiation heat transfer. Conduction is the transfer of heat by molecular motion within a solid medium. Figure 1 shows these types of heat transfer. The rate of radiant energy transfer is given by the Stefan–Boltzmann Law [6]:

$$E_r = \varepsilon \sigma T^4 \qquad (1)$$

By conservation of momentum, the thermal force or rate of change of momentum for a radiating surface element, assuming a Lambertian surface, is expressed as [5]

$$d\vec{f}_{thermal} = -\frac{2}{3} \frac{\varepsilon \sigma T_a^4}{c} \, dA \hat{n}_a \qquad (2)$$

The unit vector in Eq. (2) is defined as normal to and directed out of the sun-tracking surface of the solar panel. The differential force must be integrated over the entire surface to determine the complete thermal force:

$$\vec{f}_{thermal} = -\frac{2\sigma}{3c} \int_\Omega \varepsilon T_a^4 \, dA \hat{n}_a \qquad (3)$$

Clearly, thermal forces cannot be computed unless spacecraft surface temperatures are known. In general, the temperature at any point within a body satisfies the heat equation [5]

$$K \nabla^2 T = \rho \, C_p \frac{\partial T}{\partial t} \qquad (4)$$

The solution to this second-order partial differential equation requires that boundary conditions be specified. The boundary conditions are defined by thermal radiation and heat conduction. As given by the conservation of energy principle, the total amount of energy coming into a surface is equal to the total amount of energy leaving the surface, assuming there is no internally generated or stored energy (no sinks and no sources). The boundary condition for the satellite surface can be obtained by expressing this condition as

$$q_{in} = q_{out} \qquad (5)$$

where q_{in} is the amount of incoming radiative energy due to external sources and internal conduction, and q_{out} is the amount of radiative energy leaving the boundary due to reradiation and conduction. Figure 2 shows the conservation of energy principle for a satellite solar panel surface. Using this concept, the boundary conditions for each surface were constructed. The incident radiative solar energy received per unit area per unit time by side a and side b of the solar panel are represented by h_a and h_b [5].

$$KA\frac{\partial T_b}{\partial X} = \varepsilon_b \sigma A T_b^4 - h_b A \qquad (6a)$$

$$-KA\frac{\partial T_a}{\partial X} = \varepsilon_a \sigma A T_a^4 - h_a A \qquad (6b)$$

The actual amount of incident radiative energy received by each side of the solar panel is a function of panel orientation and the orbit of the satellite. The subscript a represents the left boundary in local coordinates (cold side), and the subscript b represents the right boundary, which, for a GPS-type satellite, is assumed to be continuously facing the sun during orbit. The term on the left side of the equal sign in Eqs. (6a) and (6b) is the heat flux, energy per unit time per unit area, in the local x-direction, which is perpendicular to the solar panel face. The values used for some of the parameters described above are listed in Table 1 and are consistent with values used for GPS satellites.

PDE-Protran, a finite element method program, was used to solve the transient heat conduction and radiation problem presented here. PDE-Protran was developed by Granville Sewell and is a general-purpose two-dimensional partial differential equation solver [7]. This software was combined with a program which incorporated material properties, the satellite's orbit orientation, and thermal environment to determine solar panel surface temperatures.

Grid points were chosen to divide the solar panel into small sections or "elements," where the temperature of the solar panel was computed for each grid point in one dimension, across the thickness of the solar panel. These grid points coincide with the boundaries between each layer of the solar panel's "sandwiched" materials (listed in Table 2). Accurate and current knowledge of physical parameters such as surface emissivity, thermal conductivity, heat capacity, and material density is required. For this analysis, the material properties are assumed to remain constant throughout the satellite's orbit, and only the solar radiation environment varies with time as the satellite experiences eclipsing or shadowing from the sun by the Earth. The material parameters directly influence the thermal forces which are calculated and have an effect on the prediction and propagation of the spacecraft trajectory. Also, these material properties may change in time or degrade, due to the harsh environment of space.[1]

III. Orbit Analysis Technique

In this investigation, the equations of motion for an Earth satellite are assumed to include the two-body gravitational effect and the thermal imbalance forces only, and are given in vector form by

$$\ddot{\vec{r}} = -\frac{\mu \vec{r}}{r^3} + \frac{\vec{f}_{\text{thermal}}}{m} \qquad (7)$$

and thermal imbalance force perturbing the satellite, $\vec{f}_{\text{thermal}}$, is computed as

$$\vec{f}_{\text{thermal}} = \frac{2\sigma A}{3c} \left(\varepsilon_b T_b^4 - \varepsilon_a T_a^4 \right) \hat{n}_a \qquad (8)$$

The effect of the thermal imbalance force on a satellite can be observed by comparing the perturbed orbit with the unperturbed two-body orbit in time. Since there is no closed-form analytical solution for the perturbed equations of motion, a numerical integration technique was necessary to solve the ordinary differential equations of motion. Because the perturbed and unperturbed orbits originate with the same initial conditions, the displacement between them at a given time can be observed. A least-squares estimation technique is used to determine the state of the satellite in its orbit at a specified epoch [8]. The initial conditions of one orbit can be adjusted at a given time to eliminate the secular divergence between the perturbed

and unperturbed orbits to observe the periodic behavior. In this analysis, two types of GPS satellite orbits were studied. The satellites of the GPS are distributed in six, evenly spaced orbit planes. When completed, the final constellation will consist of 24 satellites at an orbit altitude of approximately 20,000 km, with an orbit period of about 12 hr. In this constellation, most satellites are exposed to full sunlight. As the orbit geometry changes, however, some GPS satellites will experience eclipsing or shadowing from the sun by the Earth. Both eclipsing and noneclipsing satellites are the focus of this study. Throughout its orbit, the GPS solar panel maintains a fixed orientation toward the sun. Nodal motion was not considered, since it is not significant for the short time interval (1 week) used in this study. No internally generated energy was modeled in this study, but the absorbed solar radiation that is converted to electricity was modeled, using the efficiency of the solar panel at 14.1 percent. Although studies have shown that for a TOPEX/POSEIDON satellite the thermal radiation forces originating with the spacecraft body are twice those from the spacecraft solar panels, the major source for thermal reradiation forces on a GPS-like satellite is the spacecraft's thin, large, solar panels [2,5]. Consequently, in this analysis, the GPS satellite's main body was not considered. Other studies are currently considering this problem of modeling thermal reradiation forces for a complete GPS spacecraft.

IV. Discussion of Results

In order to determine the direction and magnitude of the thermal force, the surface temperatures were calculated using the finite element method program, PDE-Protran [7]. Several simulations were tested. The input required for the simulation is shown in Table 2. This table lists the material properties for a Block II GPS satellite solar panel [9,11].[2-5] The initial conditions included a solar panel orientation perpendicular to the sun and an initial temperature of 300 K. The time step used in the analysis was 100 sec (one GPS orbit is approximately 43,200 sec, and the eclipsing period lasts approximately 3200 sec).

GPS satellites experience an eclipsing season for only a few weeks every year. Eclipsing has a strong effect on the solar radiation environment of those satellites. This is

[1] T. T. Lam, personal communication, Aerospace Corporation, El Segundo, California, May 1990.

[2] Ibid.

[3] W. Pence, personal communication, Rockwell International, Seal Beach, California, October 1990.

[4] J. Albeck, personal communication, Spectrolab Corporation, Sylmar, California, August 1990.

[5] D. Marvin, personal communication, Aerospace Corporation, El Segundo, California, January 1991.

evident in the temperature of a GPS satellite solar panel over one orbit, as shown in Fig. 3. The steady-state temperature for the sun-facing side is approximately 317 K, and for the shaded side it is 313 K. These values compare well with the approximate value of 313 K, which has been measured on the cold, shaded side of the solar panel for a GPS satellite.[6,7] The face exposed to the sun has not been directly measured and, therefore, the temperature difference between the surfaces is not well known, but is believed to be approximately 5 K [10].[8-10] During the eclipse period, which lasts approximately 1 hr, panel temperature declines approximately 253 K. After exiting the shadow region, the solar panels slowly return to their steady-state temperatures over approximately 3 hr.

Modeling the cover-glass surface accurately has been difficult during this study since data on the properties of this surface were not readily available. The thermal conductivity of this fused silica layer is very low as compared to that of two other dominant layers, the aluminum core and the solar cell layers.[11] The cover-glass layer, on the sun-facing side of the solar panel, contributes most of the temperature imbalance, primarily because of its low thermal conductivity and greater thickness as compared to other solar panel layers, especially the aluminum core. Although it is believed that the solar panel cover-glass layer is transparent to all incident radiation, the material properties of this specific layer of the solar panel were not deleted from this analysis. It was important to simulate the solar panel as it exists in orbit to observe the long-term orbital effects of the thermal imbalance force on a GPS satellite. This simulation is adequate as long as the correct material properties are used in the analysis.

As an example, two simulations were performed using identical solar panel parameters (values given in Table 2) except for different thermal conductivities for the sun-facing cover-glass layer. These simulations are presented to show the sensitivity of the temperature calculations to the thermal conductivity of the cover glass. The value for the thermal conductivity given in test case 2, shown in Table 3, was used to demonstrate how unrealistic thermal forces can be computed when using incorrect values for the solar panel material properties. Previously, however, this was believed to be the correct value for the thermal conductivity of the fused silica cover-glass layer of a GPS

satellite solar panel [9].[12] The results, shown in Table 3, describe the steady-state temperatures and thermal accelerations that were computed using the specified values for the cover-glass thermal conductivity. Again, both test cases shown in Table 3 are identical except for the value of thermal conductivity for the solar panel cover-glass layer.

In this article, the reference frame is defined as spacecraft-centered radial and along-track components. The along-track component is also referred to as the transverse or down-track direction, defined in the direction of the satellite velocity vector. Figure 4 shows radial and along-track components of the acceleration due to thermal reradiation over one orbit for an eclipsing satellite. These components compare well with those of studies which have shown unmodeled nongravitational forces to cause errors of the magnitudes shown in Fig. 4 [10]. Also, these results were computed using the information presented in Table 2 and described as test case 1 in Table 3.

Figure 5 shows the differences between two orbits, one computed using two-body effects only and the other—an eclipsing orbit—computed with two-body effects and the thermal imbalance force during 1 week. The radial rms is 0.5 m, and the along-track rms is 5.2 m. These results were computed using a technique similar to the method used to predict satellite orbits based on a set of initial conditions and a complete force model of the spacecraft, which could include the solar radiation pressure and thermal imbalance force. In the case of the eclipsing satellite after 7 days, the along-track components differ by approximately 13 m.

Figure 6 also shows the differences between two orbits, one computed using two-body effects only and the other computed using two-body effects and the thermal imbalance force for a satellite not in an eclipsing plane. The radial rms is 0.5 m, and the along-track rms is 1.6 m. It can be seen from these results that an eclipsing satellite experiences a larger perturbation in the along-track direction over the span of 1 week than a satellite not in an eclipsing orbit plane. For the noneclipsing satellite after 7 days, the along-track difference is approximately 5 m.

Figures 7 and 8 represent the results computed using a least-squares estimation algorithm in which the simulated observation data contained only the two-body gravitational and thermal imbalance reradiation forces. The force model used in the estimation algorithm contained the two-body gravitational force model and a solar radiation pressure model to observe the ability of the force model to account for thermal imbalance forces which have

[6] Pence, op. cit.

[7] Albeck, op. cit.

[8] Pence, op. cit.

[9] Albeck, op. cit.

[10] Marvin, op. cit.

[11] Ibid.

[12] Lam, op. cit.

been difficult to model but exist in the observations. The calculated best estimate of the satellite epoch state, in the least squares sense, includes the satellite position, velocity, and a solar-radiation pressure scale factor.

Figure 7 shows the orbit fit residuals for a satellite in an orbit plane that is regularly eclipsing. The radial rms is 5 cm, and the along-track rms is 80 cm. After 7 days, the along-track orbit error is almost 2 m. These results show that the solar-radiation pressure scale factor in the estimation scheme is capable of absorbing most of the orbit error due to thermal reradiation, but not all of the orbit error, especially in the along-track direction.

Figure 8 also shows orbit fit residuals for a GPS satellite using the same estimation technique, but for a satellite in a noneclipsing orbit plane. The radial rms is 9 mm, and the along-track rms is 17 cm. After 7 days, the along-track orbit error is approximately 40 cm. Clearly, the eclipsing of the satellites has an influence on the orbit errors when a thermal reradiation force is not included in the estimation force model. Larger orbit errors are calculated when the satellite is in an eclipsing orbit plane. A 1-week prediction can be made using the satellite state computed for the best least squares estimate in Fig. 7 and compared to the best least squares estimate for that predicted week. Studies have shown that, for eclipsing satellites, the quadratic-like growth in the along-track direction can give errors as large as 50 m after a 1-week prediction [12].

V. Concluding Remarks

The current analysis has shown that orbit errors larger than 10 m occur when mismodeling nongravitational forces such as the thermal imbalance force presented here. A finite element method technique has been used to calculate satellite solar panel temperatures which are used to determine the magnitude and direction of the thermal imbalance force. Although this force may not be responsible for all of the force mismodeling, conditions may work in combination with the thermal imbalance force to produce accelerations on the order of 1.0×10^9 m/sec^2. One possible contribution currently being studied is the solar

panel misalignment acting together with the thermal imbalance force, a contribution that may account for much of the unmodeled perturbations. If submeter-accurate orbits and centimeter-level accuracy for geophysical applications are desired, a time-dependent model of the thermal imbalance force should be used, especially when satellites are eclipsing and the observed errors are larger than those for satellites in noneclipsing orbits. One study has shown that estimating additional stochastic solar radiation parameters improves GPS orbit accuracy significantly, especially for eclipsing satellites [13]. This technique can be used to absorb the orbit error caused by mismodeling thermal imbalance forces.

Although modeling the spacecraft solar panels alone may be considered insufficient, thermal force modeling of the entire spacecraft is a complicated problem. This has been done for spacecraft such as TOPEX/POSEIDON, where precise orbit determination is critical to mission success [2]. The study presented here, however, focused only on modeling the solar panels, where the material composition is not nearly as complex. Also, the problem of radiation absorbed and conducted through the solar panel and reradiated out is a simple one-dimensional time-dependent heat-transfer problem, with no internal heat generation from scientific instruments or electronics.

Nongravitational perturbations like the thermal imbalance force have been observed for years on satellites like LAGEOS, and are still not completely understood. Thermal forces are dependent on the environment and specifically on such parameters as the satellite mass, cross-sectional area, and material composition. Unfortunately, these parameters can change or degrade with long-term exposure in space. For this reason, it may be more appropriate to estimate stochastic force parameters to represent the thermal reradiation forces since the nature and rate of material degradation of the satellite in orbit is unknown [13]. The results obtained using the finite element model in this study agree with the work of others who have conducted similar studies using the finite difference technique to determine spacecraft thermal gradient forces in an effort to improve the satellite force models.

Acknowledgments

References

[1] Y. Vigue, *Thermal Imbalance Effects on a GPS Satellite*, Technical Memorandum 90-01, University of Texas Center for Space Research, Austin, Texas, May 1990.

[2] P. G. Antreasian and G. W. Rosborough, "Prediction of Radiant Energy Forces on the TOPEX/POSEIDON Spacecraft," *Journal of Spacecraft and Rockets*, vol. 29, no. 1, pp. 81–90, January–February 1992.

[3] V. J. Slabinski, *LAGEOS Acceleration Due to Intermittent Solar Heating During Eclipse Periods*, paper no. 3.9, Gaithersburg, Maryland: American Astronomical Society, July 1988.

[4] D. P. Rubincam, *LAGEOS Orbit Decay Due to Infrared Radiation from Earth*, NASA Technical Memorandum 87804, National Aeronautics and Space Administration, Washington, DC, January 1987.

[5] R. A. Cook, *The Effects of Thermal Imbalance Forces on a Simple Spacecraft*, Technical Memorandum 89-02, University of Texas Center for Space Research, Austin, Texas, May 1989.

[6] A. J. Chapman, *Heat Transfer*, New York: Macmillan Publishing Company, p. 14, 1984.

[7] G. Sewell, *Analysis of a Finite Element Method: PDE/Protran*, New York: Springer–Verlag, 1985.

[8] B. Tapley, "Statistical Orbit Determination Theory," *Recent Advances In Dynamical Astronomy*, edited by B. Tapley and V. Szebehely, August 1972.

[9] Y. Vigue, *Recent Work on the Effects of Thermal Imbalance Forces on a GPS Satellite*, Technical Memorandum 90-02, University of Texas Center for Space Research, Austin, Texas, p. 5, May 1990.

[10] H. F. Fliegel, T. E. Gallini, and E. R. Swift, "Global Positioning System Radiation Force Model for Geodetic Applications," *Journal of Geophysical Research*, vol. 97, no. B1, pp. 559–568, January 1992.

[11] H. S. Rauschenbach, *Solar Cell Array Design Handbook*, New York: Van Nostrand–Reinhold Company, pp. 467–468 and 493, 1980.

[12] B. Schutz, C. S. Ho, P. A. M. Abusali, and B. D. Tapley, "Casa Uno GPS Orbit and Baseline Experiments," *Geophysical Research Letters*, vol. 17, no. 5, pp. 643–646, April 1990.

[13] Y. Vigue, S. M. Lichten, R. J. Muellerschoen, G. Blewitt, and M. B. Heflin, "Improved Treatment of GPS Force Parameters in Precise Orbit Determination Applications," AAS paper no. 93-159, Pasadena, California, February 1993.

Appendix

Glossary

Character	Purpose and/or usage
A	surface area
c	speed of light
C_p	specific heat
E_r	energy emitted by a real body, summed over all wavelengths
$\vec{f}$	thermal imbalance force per unit area
h	incident solar radiation received by solar panel
K	thermal conductivity
m	satellite mass, kg
$\hat{n}$	unit vector normal to surface of solar panel
q	radiative energy
$\vec{r}$	geocentric satellite position vector
r	radial distance from Earth's center of mass to satellite
t	time
T	temperature
α	surface absorptivity
ε	emissivity
ρ	density
Ψ	solar constant
σ	Stefan–Boltzmann constant
μ	Earth's gravitational parameter

Subscript	
a	solar panel sun-tracking front side
b	solar panel back side, no direct sunlight
in	incoming to the spacecraft
out	leaving the body
r	radiative
thermal	thermal imbalance

Table 1. GPS thermal and orbit parameters.

Model parameter	Value
Initial orbit radius, m	26,550,000
Surface emissivity (ε_a)	0.78
Surface emissivity (ε_b)	0.83
Surface absorptivity (α_a), percent	0.77–14.1 (panel efficiency)
Solar panel surface area (A), m^2	10.832
Satellite mass (m), kg	845
Initial panel temperature $(t = 0)$, K	300
Stefan–Boltzmann constant (σ), W/m^2 K	5.6699×10^{-8}
Speed of light (c), m/sec	2.998×10^8
Solar constant (Ψ), W/m^2	1368.2
Total panel thickness (eight layers), m (in.)	0.01478 (0.582)

Table 2. GPS Block II solar panel properties.

Panel layer composition	Thickness, m	Density, kg/m^3	Specific heat, J/kgK	Conductivity, W/mK
Cover glass	0.00749	2186.622	753.624	1.417
Adhesive	0.00005	1079.472	1256.04	0.116
Solar cell	0.00025	2684.84	711.756	147.994
Interconnect cell adhesive	0.00018	1051.793	1256.04	0.116
Kapton cocured	0.000076	1162.508	1130.436	0.1506
Graphite epoxy	0.00019	2186.622	1373.27	0.8706
Aluminum core	0.00635	24.91088	1046.7	250.966
Graphite epoxy	0.00019	2186.622	1373.27	0.8706

Table 3. Cover glass thermal simulation.

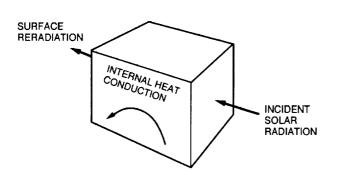| Test case 1	Test case 2
$K = 1.417$ W/mK	$K = 0.04327$ W/mK
Hot side $T_a = 317.41$ K	Hot side $T_a = 340.30$ K
Cold side $T_b = 313.66$ K	Cold side $T_b = 285.37$ K
Thermal acceleration $= 1.88 \times 10^{-10}$ m/sec^2	Thermal acceleration $= -8.01 \times 10^{-9}$ m/sec^2

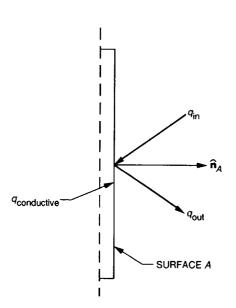Fig. 1. General heat transfer diagram for a spacecraft.

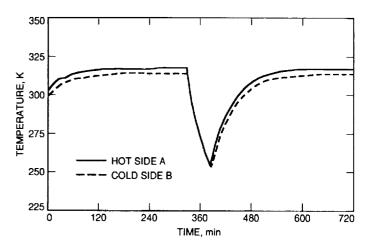Fig. 2. Conservation of energy diagram for a satellite surface.

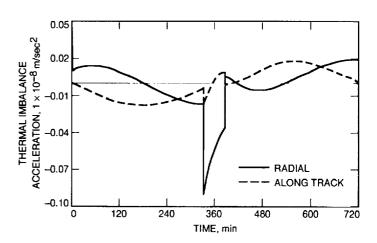Fig. 3. Temperature history simulation for a GPS solar panel.

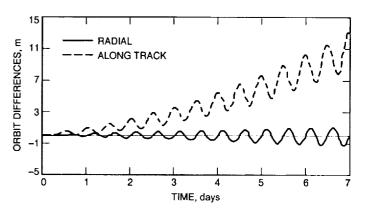Fig. 4. Radial and along-track components for the thermal force over one orbit.

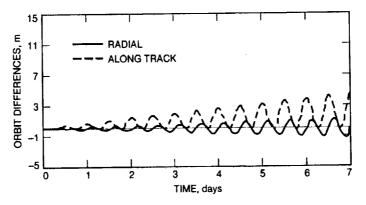Fig. 5. Radial and along-track orbit differences, eclipsing satellite.

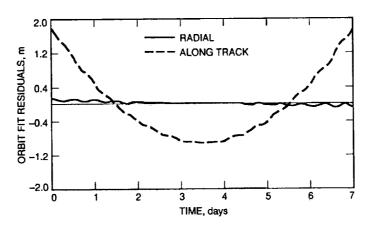**Fig. 6. Radial and along-track orbit differences, noneclipsing satellite.**

Fig. 7. Orbit fit residuals, with a solar-radiation pressure scale factor, eclipsing satellite.
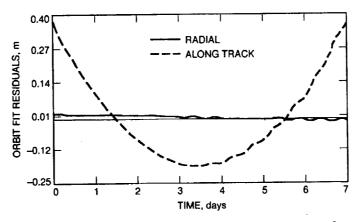

Fig. 8. Orbit fit residuals, with a solar-radiation pressure scale factor, noneclipsing satellite.